SUPPLEMENTARY INFORMATION

Mechanistic elucidation of the yttrium(III)-catalysed intramolecular aminoalkene hydroamination: DFT favours a stepwise σ-insertive mechanism

Sven Tobisch[a]

[a] *School of Chemistry, University of St Andrews, Purdie Building, North Haugh, St Andrews, KY16 9ST, United Kingdom*

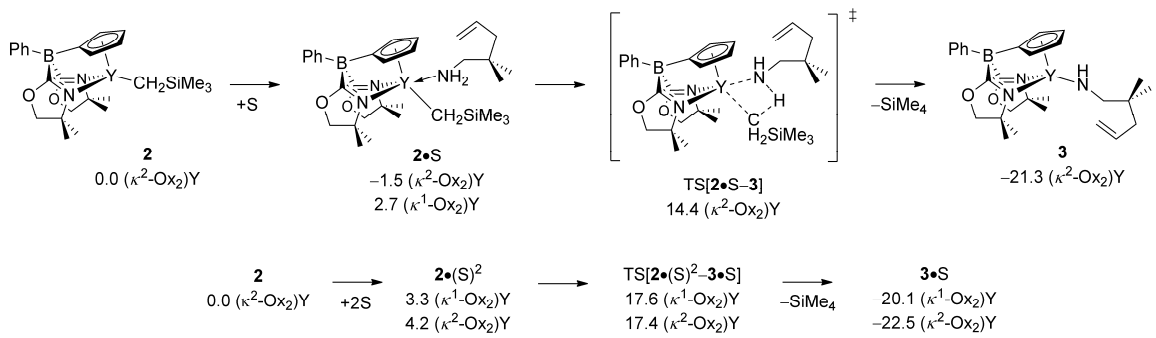

Fig. S1. Y–C bond aminolysis at **2** by substrate **1**. The $\{Cpo^{M}\}YCH_2SiMe_3$ compound **2** (with the appropriate number of substrate molecules) has been chosen as reference for relative free energies given in [kcal mol^{-1}].

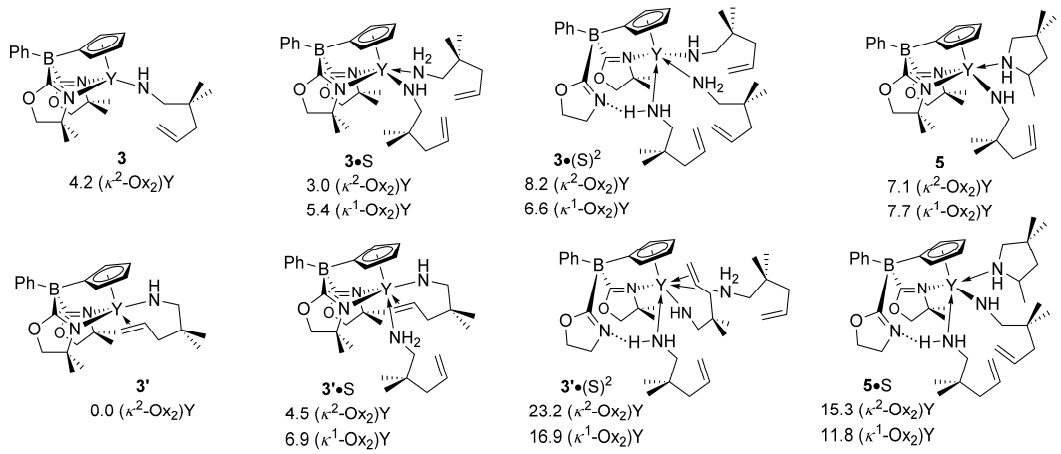

Fig. S2. Amine association at the catalytically relevant $\{Cpo^{M}\}Y$–amidoalkene compound ($\{Cpo^{M}\} = \{PhB(C_5H_4)(Ox^{Me2})_2\}$). The prevalent [$\{Cpo^{M}\}Y$–amidoalkene] species **3'** (with the appropriate number of substrate or cycloamine molecules) has been chosen as reference for relative free energies given in [kcal mol^{-1}].

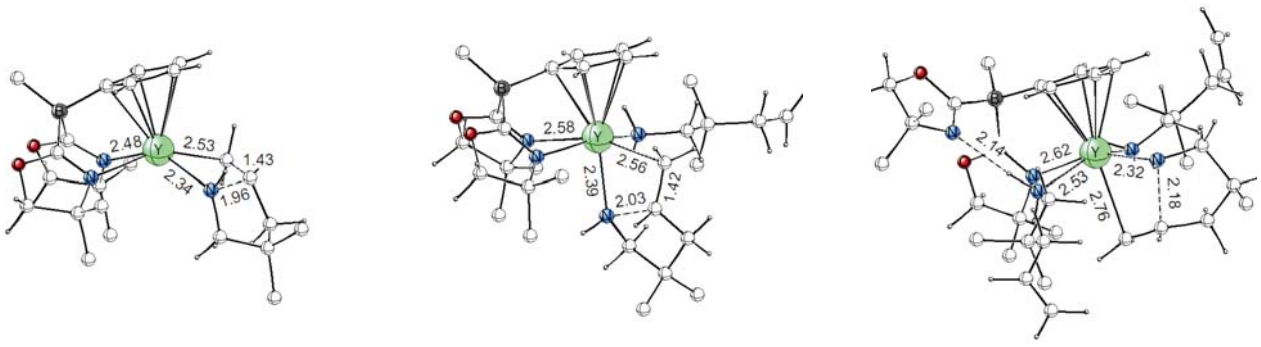

TS[**3'**–**4**] {κ^2-Ox$_2$}Y TS[**3**•S–**4**•S] {κ^2-Ox$_2$}Y TS[**3**"•(S)^2–**4**•(S)^2] {κ^1-Ox$_2$}Y

Fig. S3. Selected structural parameter (angstroms) of located TS structures for σ-insertive cyclisation through pathways without and with adducted substrate molecules involved. The methyl and phenyl groups at the {Cpo^M}Y backbone are displayed in a truncated fashion and also amino-/amidoalkene units.

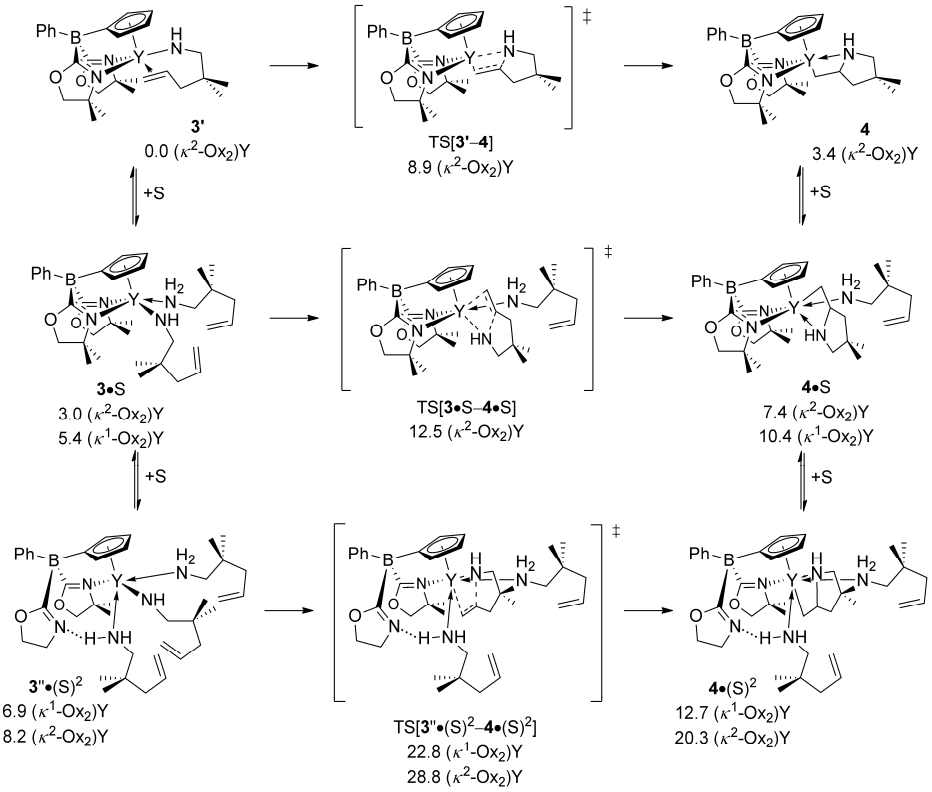

Fig. S4. Migratory olefin insertion into the Y–N amido σ-bond at **3** and its substrate adducted species **3**•S and **3**•(S)^2. The prevalent [{Cpo^M}Y–amidoalkene] species **3'** (with the appropriate number of substrate molecules) has been chosen as reference for relative free energies given in [kcal mol^{-1}].

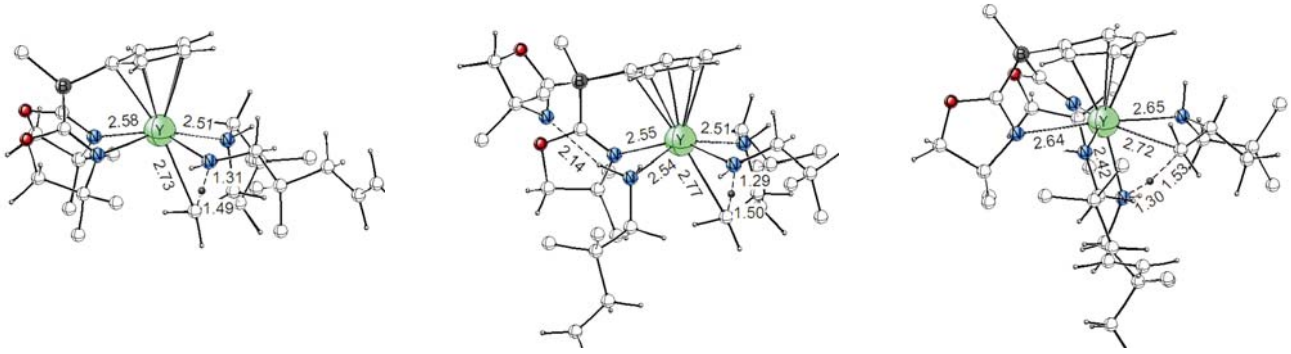

TS[**4**"•S–**5**] {κ^2-Ox$_2$}Y TS[**4**"•(S)^2–**5**•S] {κ^1-Ox$_2$}Y TS[**4**"•(S)^2–**5**•S] {κ^2-Ox$_2$}Y

Fig. S5. Selected structural parameter (angstroms) of located TS structures for protonolytic azacycle Y–C bond cleavage through pathways with one or two adducted substrate molecules involved. The methyl and phenyl groups at the {Cpo^M}Y backbone are displayed in a truncated fashion and also amino-/amidoalkene units.

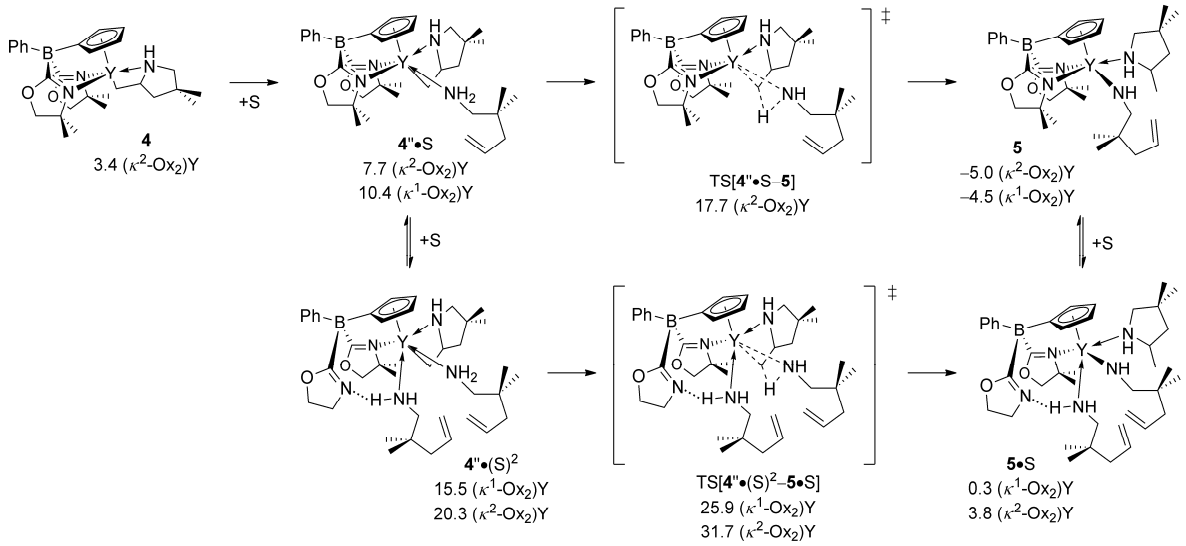

Fig. S6. Y–C azacycle tether aminolysis at the yttrium alkyl intermediate through pathways with one or two adducted substrate molecules involved. The prevalent [{Cpo^M}Y–amidoalkene] species **3'** (with the appropriate number of substrate molecules) has been chosen as reference for relative free energies given in [kcal mol^{-1}].

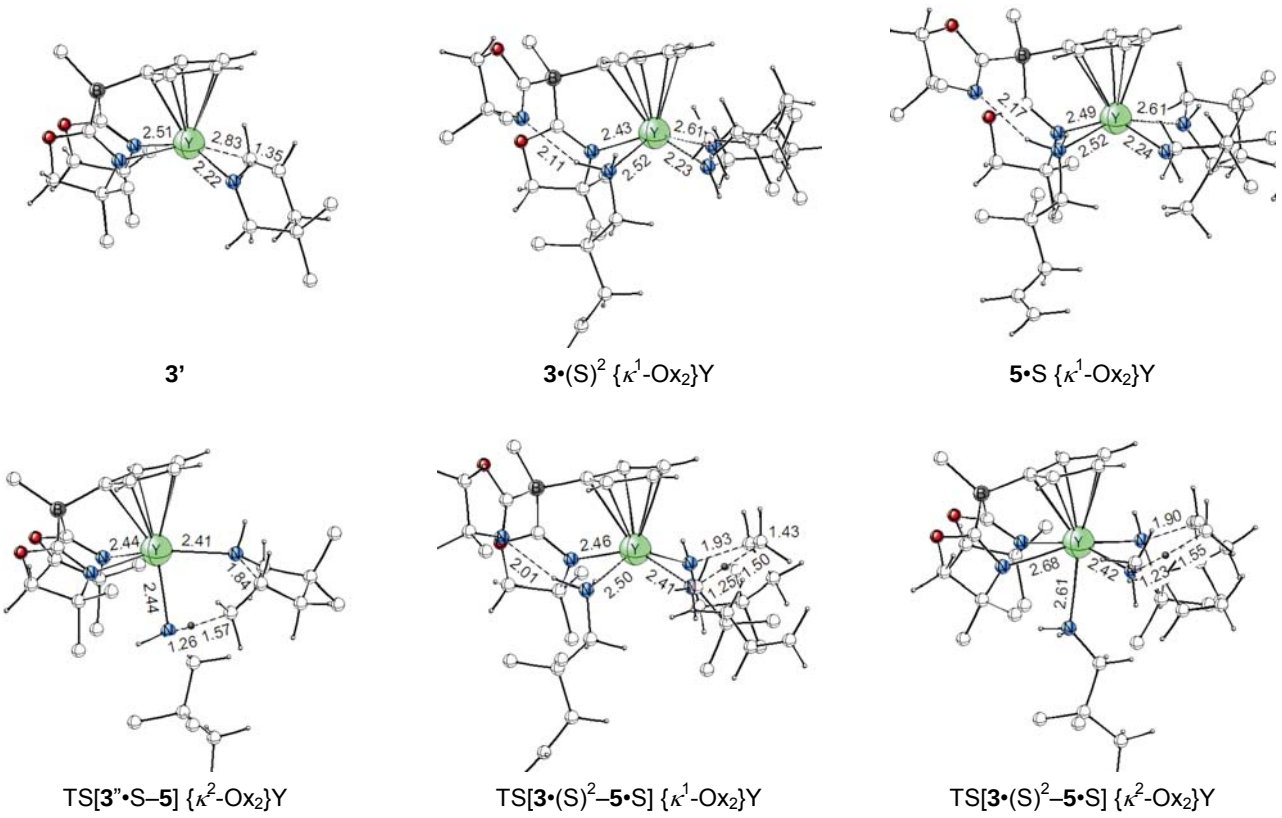

3' | **3**•(S)^2 {κ^1-Ox$_2$}Y | **5**•S {κ^1-Ox$_2$}Y

TS[**3''**•S–**5**] {κ^2-Ox$_2$}Y | TS[**3**•(S)^2–**5**•S] {κ^1-Ox$_2$}Y | TS[**3**•(S)^2–**5**•S] {κ^2-Ox$_2$}Y

Fig. S7. Selected structural parameter (angstroms) of the optimised structures of key stationary points for non-insertive N–C ring closure with concurrent amino proton transfer at the double bond at **3**•(S)^2. The methyl and phenyl groups at the {Cpo^M}Y backbone are displayed in a truncated fashion and also amino-/amidoalkene units.

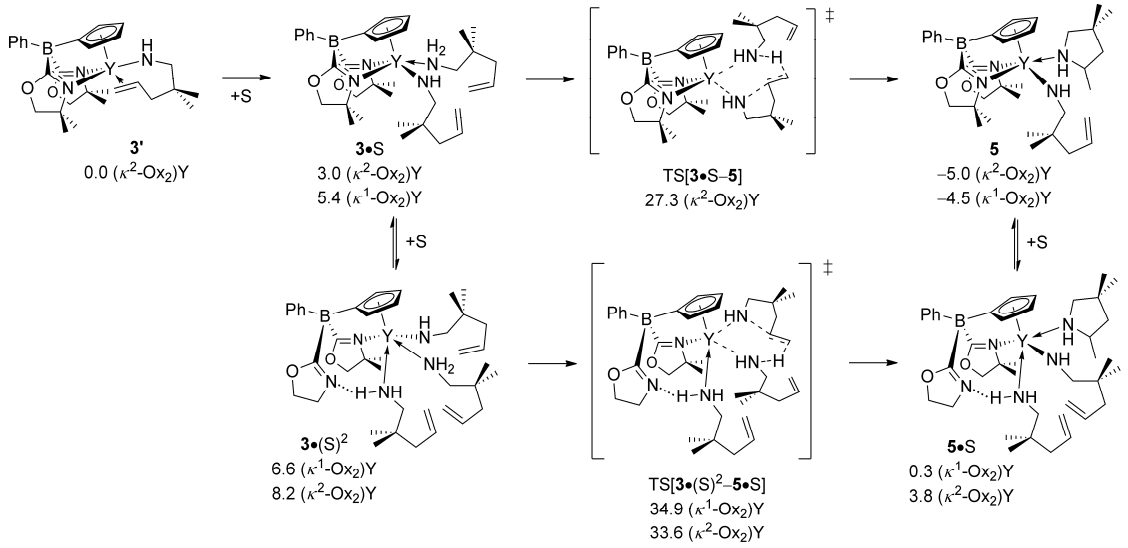

Fig. S8. Non-insertive N–C ring closure with concurrent amino proton transfer at the olefin unit at **3**•S and **3**•(S)^2. The prevalent [{Cpo^M}Y–amidoalkene] species **3'** (with the appropriate number of substrate molecules) has been chosen as reference for relative free energies given in [kcal mol^{-1}].

Computational Details

All calculations have been performed with the program package TURBOMOLE[1] using Kohn-Sham density functional theory[2] (DFT). The almost nonempirical *meta*-GGA Tao–Perdew–Staroverov–Scuseria (TPSS)[3] was used together with the RI-*J* approximation.[4] The good to excellent performance of the TPSS functional for a wide range of applications[5] and rare-earth[6] and alkaline-earth[7] element-catalysed HA in particular, has been demonstrated previously. In view of the fact that all species investigated in this study show a large HOMO−LUMO gap, a spin-restricted formalism was used for all the calculations. For Y we used the Stuttgart−Dresden scalar-relativistic pseudopotential (28MWB, 28 core electrons)[8] in combination with the (7s7p5d1f)/[6s4p3d1f] valence basis set.[9] All remaining elements were represented by Ahlrich's valence triple-ζ TZVP basis set[10a,b] with polarization functions on all atoms.

The reaction paths were explored by the growing string method,[11] in which two string fragments (commencing from reactant and product side, respectively) are grown until the two fragments join. As this was performed in mass-weighted coordinates, an approximate to the minimum energy path (MEP) was obtained. This identified the reactant and product states to be linked to the associated transition state. The approximate saddle points connected with the MEP were subjected to an exact localisation of the TS structures. The geometry optimisation and the saddle-point search were carried out by utilising analytical/numerical gradients/Hessians according to standard algorithms. No symmetry constraints were imposed in any case. The stationary points were identified exactly by the curvature of the potential-energy surface at these points corresponding to the eigenvalues of the Hessian. All reported transition states possess exactly one negative Hessian eigenvalue, while all other stationary points exhibit exclusively positive eigenvalues. The many isomers that are possible for each of the investigated species were carefully explored. It has been explicitly scrutinized for each of the individual steps as to whether additional substrate molecules, which are present in excess, are likely serving to facilitate the elementary process.

The reaction and activation enthalpies and free energies (ΔH, $\Delta H^{\ddagger}$ and ΔG, $\Delta G^{\ddagger}$ at 298 K and 1 atm) were evaluated according to standard textbook procedures[12] using computed harmonic frequencies. The frequency analysis was performed for stationary points that were located with an alternative basis set, consisting of the aforementioned basis for Y and Ahlrichs' split valence SV(P) basis set[10c] with polarisation functions on main group atoms, but not on hydrogen. This level of basis-set quality has been identified as a reliable tool for the assessment of structural parameters and vibrational frequencies,[13] thus this strategy allows an affordable and accurate determination of thermodynamic state functions. Enthalpies were reported as ΔE + zero point energy corrections at 0 K + thermal motion corrections at 298 K and Gibbs free-energies were obtained as $\Delta G = \Delta H - T\Delta S$ at 298 K.

The influence of nonspecific solute−solvent interactions[14] on both geometries and reaction energetics has been estimated for benzene (dielectric constant ε = 2.247 at 298 K)[15] by employing the conductor-like screening model (COSMO) due to Klamt and Schüürmann[16] as implemented in TURBOMOLE.[17] The solvent excluding surface was used along with ε = 2.247 and nonelectrostatic contributions to solvation were not considered. The solvation effects were included selfconsistently in the calculations, and all key stationary species were fully optimised in the presence of the bulk solvent. The optimised atomic COSMO radii (r_H = 1.3 Å, r_C = 2.0 Å, r_N = 1.83 Å, r_o = 1.72 Å)[18] have been used, in combination with the van der Waals radius[19] (multiplied by a standard scaling factor of 1.17) for boron; i.e. r_B = 2.05 Å, and a radius of 2.22 Å for Y. Although the Born energy reported by the COSMO model is, in a strict sense, a free energy, the entropy contributions accounts to only a very small fraction (~2%) of the total energy.[20] The solvation enthalpy was approximated by the difference between the electronic energy computed using the COSMO solvation model and the gas-phase energy. As an alternative, $H_{solution}(T)$ can be obtained from the same functional form as for $H_{gas}(T)$, but with the inertia moments and vibrational frequencies modified by solvation.[21] This gave almost identical results with an enthalpy disparity of typically less than 1 kcal mol^{-1}, but at drastically increased computational costs. The entropy contributions for condensed-phase conditions were estimated based on the computed gas-phase entropies by employing the procedure of Wertz.[22] According to this three step procedure, the solute in

gas phase is first compressed to the molar volume of the solvent. The associated change in solute entropy is given by $\Delta S = R \ln(V_{m,f}/V_{m,i})$, where $V_{m,i}$ and $V_{m,f}$ are the solute molar volumes at initial and final stage; thus $\Delta S_1 = R \ln(V_{m,lig}/V_{m,gas})$ for the first step. The compressed solute then loses the same fraction of its entropy, which would be lost upon transfer from gas to liquid when the two phases have the same density, namely that of the liquid. The entropy fraction α lost here is given by $\alpha = (S_{liq}^\circ - S_{gas,ligdens})/S_{gas,ligdens}$, where the entropy of gaseous solvent at the same density as the liquid $S_{gas,ligdens}$ can be obtained from $S_{gas}^\circ + R \ln(V_{m,lig}/V_{m,gas})$. In a third step, the solute gas is expanded from the molar volume of the liquid solvent to the density of a standard solution of 1.0 L mol^{-1}, with $\Delta S_3 = R \ln(V_{m,1M}/V_{m,lig})$. Taking the experimental data for benzene,[15] the entropy fraction lost in the second step amounts to $\alpha = -0.22$.[23] On assumption that all solute molecules lose the same fraction of their entropy when transferred from gas to liquid, some simple algebraic transformation leads to the solvation entropy as given by the sum of the entropy changes associated with each of the three steps, *viz*. $\Delta S_{solv} = \Delta S_1 + \alpha(S_{gas}^\circ + \Delta S_1) + \Delta S_3$. Thus, for benzene solvent at 298 K one obtains $\Delta S_{solv} = -0.22 S_{gas}^\circ - 3.92$ cal/K•mol. Accordingly, the procedure proposed by Wertz gives rise to the following estimate for the total solute entropy (again for benzene solvent at 298 K) as expressed in terms of the gas-phase entropy:

$$S_{sol} = 0.78\ S_{gas}^\circ - 3.92 \text{ cal/K•mol} \qquad (1)$$

Although somehow empirical, the Wertz procedure provides a reasonable estimate of the entropy of a molecule in condensed phase, which is known to be less than its entropy in gaseous phase,[22–24] which may be used in a somewhat pragmatic way in the absence of reliable alternatives that are affordable. Noteworthy, this procedure has been successfully applied in several cases.[25] The strict treatment of the free-energy in condensed phase, for instance by applying non-empirical MD simulation techniques, is currently too expensive to be carried out for a mechanistic scenario as diverse as explored herein and taking the size of the employed catalyst model also into account; this is likely to remain so in the foreseeable future.

1 (a) R. Ahlrichs, M. Bär, M. Häser, H. Horn and C. Kölmel, *Chem. Phys. Lett.*, 1989, **162**, 165; (b) O. Treutler and R. Ahlrichs, *J. Chem. Phys*., 1995, **102**, 346; (c) R. Ahlrichs, F. Furche, C. Hättig, W. Klopper, M. Sierka and F. Weigend, *TURBOMOLE, version 6.0*; University of Karlsruhe: Karlsruhe, Germany, 2009; http://www.turbomole.com.

2 R. G. Parr and W. Yang, W. *Density-Functional Theory of Atoms and Molecules*, Oxford University Press, 1989.

3 (a) P. A. M. Dirac, *Proc. Royal Soc. (London)*, 1929, **A123**, 714; (b) J. C. Slater, *Phys. Rev*., 1951, **81**, 385; (c) J. P. Perdew and Y. Wang, *Phys. Rev*., 1992, **B45**, 13244; (d) J. Tao, J. P. Perdew, V. N. Staroverov and G. E. Scuseria, *Phys. Rev. Lett*., 2003, **91**, 146401; (e) J. P. Perdew, J. Tao, V. N. Staroverov and G. E. Scuseria, *J. Chem. Phys*., 2004, **120**, 6898.

4 (a) O. Vahtras, J. Almlöf and M. W. Feyereisen, *Chem. Phys. Lett*., 1993, **213**, 514; (b) K. Eichkorn, O. Treutler, H. Öhm, M. Häser and R. Ahlrichs, *Chem. Phys. Lett*., 1995, **242**, 652.

5 (a) V. N. Staroveroc, G. E. Scuseria, J. Tao and J. P. Perdew, *J. Chem. Phys*., 2003, **119**, 12129; (b) I. Hyla-Kryspin and S. Grimme, *Organometallics,* 2004, **23**, 5581; (c) Y. Zhao and D. G. Truhlar, *J. Chem. Theory Comput*., 2005, **1**, 415; (d) F. Furche and J. P. Perdew, *J. Chem. Phys*., 2006, **124**, 044103; (e) F. Neese, T. Schwabe and S. Grimme, *J. Chem. Phys*., 2007, **126**, 124115; (f) M. Bühl, C. Reimann, D. A. Pantazis, T. Bredow and F. Neese, *Chem. Theor. Comput*., 2008, **4**, 1449.

6 (a) S. Tobisch, *Chem. Eur. J*. 2010, **16**, 13814; (b) S. Tobisch, *Dalton Trans*., 2011, **40**, 249.

7 S. Tobisch, *Chem. Eur. J*., 2011, **17**, 14974.

8 D. Andrae, U. Häußermann, M. Dolg, H. Stoll, H. Preuß, Theor. Chim. Acta, 1990, **77**, 123.

9 (a) F. Weigend and R. Ahlrichs, *Phys. Chem. Chem. Phys*., 2005, **7**, 3297; (b) F. Weigend, *Phys. Chem. Chem. Phys*., 2006, **8**, 1057.

10 (a) A. Schäfer, C. Huber and R. Ahlrichs, *J. Chem. Phys*., 1994, **100**, 5829; (b) K. Eichkorn, F. Weigend, O. Treutler and R. Ahlrichs, *Theor. Chem. Acc*., 1997, **97**, 119; (c) A. Schäfer, C. Huber and R. Ahlrichs, *J. Chem. Phys*., 1992, **97**, 2571.

11 (a) B. Peters, A. Heyden, A. T. Bell and A. Chakraborty, *J. Chem. Phys*., 2004, **120**, 7877; (b) A. Heyden, *personal communication*.

12 D. A. McQuarrie, *Statistical Thermodynamics*, Harper & Row, New York, 1973.

13 W. Koch and M. C. Holthausen, *A Chemist's Guide to Density Functional Theory*, 2nd Ed., Wiley-VCH, Weinheim, 2001.

14 (a) J. Tomasi and M. Persico, *Chem. Rev*., 1994, **94**, 2027; (b) C. J. Cramer and D. G. Truhlar, *Chem. Rev*., 1999, **99**, 2161; (c) C. J. Cramer, *Essentials of Computational Chemistry: Theories and Models*; John Wiley & Sons : Chincester, U.K., 2002, pp 347–383.

15 *CRC Handbook of Chemistry and Physics* (Ed.: D. R. Lide), 84th ed. CRC Press, New York, 2003–2004.

16 (a) A. Klamt and G. Schüürmann, *J. Chem. Soc. Perkin Trans. 2*, 1993, 799; (b) A. Klamt, in *Encyclopaedia of Computational Chemistry* (Ed,: P. v. R. Schleyer), John Wiley, & Sons: Chichester, 1998; Vol. 1, pp. 604 –615.
17 A. Schäfer, A. Klamt, D. Sattel, J. C. W. Lohrenz and F. Eckert, *Phys. Chem. Chem. Phys*., 2000, **2**, 2187.
18 A. Klamt, V. Jonas, Th. Bürger and J. C. W. Lohrenz, *J. Phys. Chem. A*, 1998, **102**, 5074.
19 A. Bondi, *J. Phys. Chem.*, 1964, **68**, 441.
20 W. E. Dasent, *Inorganic Energetics*, Penguin, Middlesex, UK, 1970.
21 A. Klamt, *J. Phys. Chem*., 1996, **100**, 3349.
22 D. H. Wertz, *J. Am. Chem. Soc*., 1980, **102**, 5316.
23 M. H. Abraham, *J. Am. Chem. Soc*., 1981, **103**, 6742.
24 (a) V. Cabani, P. Gianni, V. Mollica and L. Lepori, *J. Solution Chem*., 1981, **10**, 563; (b) D. D. Wagman, W. H. Evans, V. B. Parker, R. H. Schumm, I. Halow, S. M. Bailey, K. L. Churney and R. L. Nuttall, *J. Phys. Ref. Data*, 1982, **11**, Supplement No. 2; (c) A. Ben-Naim and Y. Marcus, *J. Chem. Phys*., 1984, **81**, 2016; (d) Y. Okuno, *Chem. Eur. J*., 1997, **3**, 212; (e) W. R. Fawcett, *J. Phys. Chem. B*, 1999, **103**, 11181.
25 (a) I. H. Williams, D. Spangler, D. A. Femec, G. M. Maggiora and R. L. Schowen, *J. Am. Chem. Soc*., 1983, **105**, 31; (b) I. H. Williams, *J. Am. Chem. Soc*., 1987, **109**, 6299; (c) S. Wolfe, Ch-K. Kim, K. Yang and N. Weinberg, Z. Shi, *J. Am. Chem. Soc*., 1995, **117**, 4240; (d) J. Cooper and T. Ziegler, *Inorg. Chem*., 2002, **41**, 6614; (e) I. H. Hristov and T. Ziegler, *Organometallics*, 2003, **22**, 3515; (f) J. K.-C. Lau and D. V. Deubel, *Chem. Eur. J*., 2005, **11**, 2849; (g) S.-T.Lin, P. K. Maiti and W. A. Goddard, III, *J. Phys. Chem. B*, 2005, **109**, 8663; (f) H. Zhu and T. Ziegler, *J. Organomet. Chem*., 2006, **691**, 4486; (h) J. K.-C. Lau and D. V. Deubel, *J. Chem. Theory Comp*., 2006, **2**, 103; (i) D. V. Deubel, *J. Am. Chem. Soc*., 2006, **128**, 1654.
26 S. S. Glad and F. Jensen, *J. Phys. Chem.*, 1996, **100**, 227.
27 C. J. Cramer, *Essentials of Computational Chemistry*, 2nd ed., John Wiley & Sons Ltd., Chichester, 2004.
28 R. T. Skodje, D. G.; Truhlar and B. C. Garrett, *J. Phys. Chem.* 1981, **85**, 3019.

Rate law derived from the assessed free-energy profile for the operative σ-insertive mechanism

$[\mathbf{3}\bullet S] = K_1[\mathbf{3'}][S]$

$[\mathbf{3}\bullet(S)^2] = K_2[\mathbf{3}\bullet S][S]$
$= K_1K_2\times[\mathbf{3'}][S]^2$

$[\mathbf{4}] = K_3[\mathbf{3'}]$

rate = $k_5[\mathbf{4''}\bullet S]$

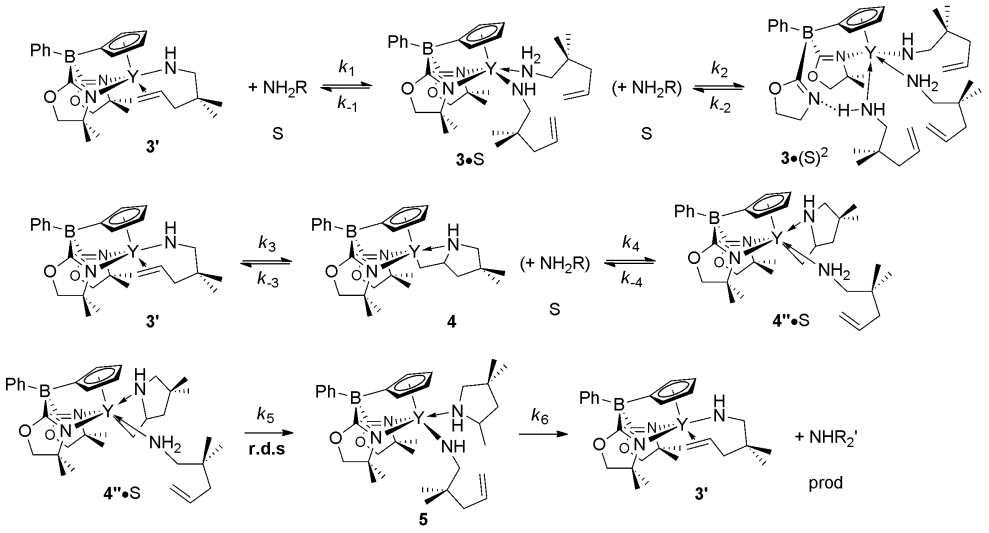

application of the steady-state approximation to **4”**•S that is formed in a sequence of reversible steps from the Y–amidoalkene catalyst species **3’**

all steps are reversible, with the exception of irreversible turnover-limiting aminolysis (k_5) and product liberation (k_6)

$d[\mathbf{4''}\bullet S]/dt = k_4[\mathbf{4}][S] - [\mathbf{4''}\bullet S](k_{-4}+k_5) =! 0$

total catalyst concentration
let $[cat]_0 = [\mathbf{3'}] + [\mathbf{3}\bullet S] + [\mathbf{3}\bullet(S)^2] + [\mathbf{4}] + [\mathbf{4''}\bullet S]$
therefore $[\mathbf{4}] = [cat]_0 - [\mathbf{3'}] - [\mathbf{3}\bullet S] - [\mathbf{3}\bullet(S)^2] - [\mathbf{4''}\bullet S]$

$d[\mathbf{4''}\bullet S]/dt = k_4[S]\times([cat]_0 - [\mathbf{3'}] - [\mathbf{3}\bullet S] - [\mathbf{3}\bullet(S)^2] - [\mathbf{4''}\bullet S]) - [\mathbf{4''}\bullet S](k_{-4}+k_5) =! 0$

$k_4[cat]_0[S] = k_4([\mathbf{3'}] + [\mathbf{3}\bullet S] + [\mathbf{3}\bullet(S)^2])[S] + k_4[\mathbf{4''}\bullet S][S] + [\mathbf{4''}\bullet S](k_{-4}+k_5)$

$[cat]_0[S] = ([\mathbf{3'}] + [\mathbf{3}\bullet S] + [\mathbf{3}\bullet(S)^2])[S] + [\mathbf{4''}\bullet S]([S] + (k_{-4}+k_5)/k_4)$

$\Rightarrow [\mathbf{4''}\bullet S] = [cat]_0[S]/(K'+[S]) - [\mathbf{3'}][S]\times(1+K_1[S]+K_1K_2[S]^2)/(K'+[S])$ with $K' = (k_{-4}+k_5)/k_4$

rate $= k_5[\mathbf{4''}\bullet S]$
$= k_5[cat]_0[S]/(K'+[S]) - k_5[\mathbf{3'}][S](1+K_1[S]+K_1K_2[S]^2)/(K'+[S])$ with $K' = (k_{-4}+k_5)/k_4$

- the derived rate law is consistent with obtained empirical rate law: $-d[sub]/dt = k'_{obs}[cat]^1[sub]^1$
- the second term in the simplified rate law accounts for substrate inhibition through reversible substrate association at the Y–amidoalkene catalyst species **3’**
- a term representing product association equilibria with **3’** can be introduced in a similar fashion to account for product inhibition

Estimation of the primary kinetic isotope effects (KIEs)

Kinetic isotope effects (KIEs) on proton transfer steps (k_{NH}/k_{ND} or k_{CH}/k_{CD}) were evaluated according to Equation 1 by using assessed zero-point-vibrational energies (ZPVEs) and partition function values as proposed by Jensen.[26,27] The partition function ratios for translation, rotation, and excited vibrational states are expressed in Equation (1) as Q^{R} and Q^{R^*} for the isotope reactants and as Q^{TS} and Q^{TS^*} for the isotopic transition states. The exponential factor gives the contribution to the kinetic isotope effect from zero-energy energy changes between isotopic reactants and transition states. Primary isotope effects tends to be dominated by the difference in zero-point-vibrational energies.

$$\mathrm{KIE} = \left(\frac{Q^{\mathrm{TS}}}{Q^{\mathrm{TS}^*}}\right)\left(\frac{Q^{\mathrm{R}^*}}{Q^{\mathrm{R}}}\right) \mathrm{e}^{-(\Delta\Delta \mathrm{ZPVE}/RT)} \qquad (1)$$

Vibrational frequencies were treated as harmonic in nature. Quantum chemical tunneling is known to play a critical role in obtaining accurate rate coefficients for proton transfer processes, especially at lower temperature, and therefore the zero curvature tunneling approximation by Skodje and Truhlar has been applied. [28] The Skodje and Truhlar approximation uses the imaginary frequency and also of the height of the potential energy barrier for estimating tunneling corrections to the transmission coefficient $\kappa(T)$ {$k_{obs} = \kappa(T)k_{class}$} according to the following analytic expressions:

$$\kappa(T) = \begin{cases} \dfrac{\beta}{\beta - \alpha}\{e^{[(\beta-\alpha)(\Delta V^{\ddagger} - V)]} - 1\} & \alpha \le \beta \\ \dfrac{\beta\pi/\alpha}{\sin(\beta\pi/\alpha)} - \dfrac{\beta}{\alpha - \beta} e^{[(\beta-\alpha)(\Delta V^{\ddagger} - V)]} & \alpha \ge \beta \end{cases}$$

with $\alpha = 2\pi/[h\ \mathrm{Im}(\nu^{\ddagger})]$ and $\beta = (k_B T)^{-1}$.

$\Delta V^{\ddagger}$ is the zero-point-including barrier, V is the zero-point-including potential-energy difference between reactants and products and $\mathrm{Im}(\nu^{\ddagger})$ is the (scaled) magnitude of the imaginary vibration.